ACS Infectious Diseases

pubs.acs.org/journal/aidcbc

Article

# Triazole-Bridged Peptides with Enhanced Antimicrobial Activity and Potency against Pathogenic Bacteria

Joshua Grabeck,[†] Jacob Mayer,[†] Axel Miltz, Michele Casoria, Michael Quagliata, Denise Meinberger, Andreas R. Klatt, Isabelle Wielert, Berenike Maier, Anna Maria Papini, and Ines Neundorf*

Cite This: https://doi.org/10.1021/acsinfecdis.4c00078

Read Online

ACCESS | Metrics & More | Article Recommendations | Supporting Information

**ABSTRACT:** There are still no linear antimicrobial peptides (AMPs) available as a treatment option against bacterial infections. This is caused by several drawbacks that come with AMPs such as limited proteolytic stability and low selectivity against human cells. In this work, we screened a small library of rationally designed new peptides based on the cell-penetrating peptide sC18* toward their antimicrobial activity. We identified several effective novel AMPs and chose one out of this group to further increase its potency. Therefore, we introduced a triazole bridge at different positions to provide a preformed helical structure, assuming that this modification would improve (i) proteolytic stability and (ii) membrane activity. Indeed, placing the triazole bridge within the hydrophilic part of the linear analogue highly increased membrane activity as well as stability against enzymatic digestion. The new peptides, 8A and 8B, demonstrated high activity against several bacterial species tested including pathogenic *N. gonorrhoeae* and methicillin-resistant *S. aureus*. Since they exhibited significantly good tolerability against human fibroblast and blood cells, these novel peptides offer true alternatives for future clinical applications and are worth studying in more detail.

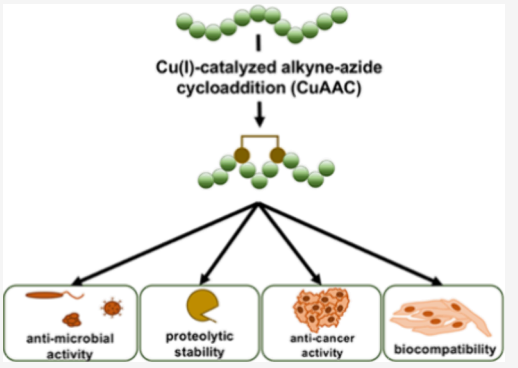


**KEYWORDS:** *antimicrobial peptides, antibacterial resistance, click-reaction, membrane activity*



Antimicrobial infections cause millions of deaths per year worldwide and are a major burden to the health care system. In addition, the rapidly growing frequency of antibiotic resistance and the decline in the discovery of new antibiotics have accelerated the need for novel treatment strategies.[1,2] Antimicrobial peptides (AMPs) have been considered as potential alternatives to combat bacterial infections.[3] They are abundant in virtually all domains of life and are representatives of the innate immune system. There, they act as a first line of defense against invading pathogens and can control infections through their microbicidal and immunomodulating properties.[4] AMPs hold great promise as they possess broad-spectrum efficacies against bacteria, fungi, and viruses[5] including multidrug resistant pathogens, such as members of the ESKAPE pathogens (*Enterococcus faecium*, *Staphylococcus aureus*, *Klebsiella pneumoniae*, *Acinetobacter baumannii*, *Pseudomonas aeruginosa*, and *Enterobacter* species).[6]

The mode of action of most cationic and amphipathic AMPs involves membrane disruptive processes or pore formation resulting in lysis of the bacterial cell membrane.[7] Owing to their cationic character, AMPs are attracted to negatively charged constituents of the bacterial surface layers. As soon as they approach the lipid phase of the bacterial membrane, they get structured and often form into an amphipathic helix.[8] Subsequently, peptide aggregation or self-assembly occurs and induces membrane perturbating effects leading in most cases to cell death.[9] On the other side, AMPs may also internalize into bacterial cells, where they interact with intracellular targets.[10]

Despite numerous advantages of AMPs, their development as drugs in human medicine is hampered by several obstacles, such as limited safety profiles, selectivity, and lability to proteolytic degradation. Hence, many researchers focus on the optimization of AMPs to design modified peptides with improved biological properties.[11] In this respect, the incorporation of unnatural building blocks has gained much interest.[12,13]

Another class of membrane-active peptides is represented by the cell-penetrating peptides (CPPs) that have been developed to interact with mammalian cells where they are used as efficient carrier systems.[14] For instance, in our group, we have established the CPP sC18 and variants thereof as drug delivery vehicles for several different applications.[15−17] In previous studies, antibiotic activity was also reported for this class of

**Received:** January 26, 2024
**Revised:** June 1, 2024
**Accepted:** June 3, 2024

**Table 1. Names, Amino Acid Sequences, Molecular Weights (MWs), Net Charges, Hydrophobicity as Measured as Retention Time by HPLC and Half Maximal Effective Concentration ($EC_{50}$) and Tested against *B. spizizenii***

| Name | Sequence | $MW_{calc.}$ [Da] | $MW_{exp.}$ [Da] | Net Charge | Hydrophobicity | $EC_{50}$ [$\mu$M] *B. spizizenii* |
|---|---|---|---|---|---|---|
| RL-1 | RLRKRLRKFRNK | 1671.08 | 1670.73 | +9 | 16.3 | 25 |
| RL-2 | GLRKLLRKFRNK | 1528.91 | 1528.42 | +7 | 19.5 | >50 |
| RL-3 | GLRKRLRKFLNK | 1528.91 | 1528.37 | +7 | 19.5 | >50 |
| RL-4 | GLRKRLRKFRRK | 1614.03 | 1613.44 | +9 | 16.2 | >50 |
| RL-5 | RLRKLLRKFRNK | 1628.05 | 1627.50 | +8 | 17.4 | >50 |
| RL-6 | RLRKRLRKFLNK | 1628.05 | 1627.48 | +8 | 17.6 | >50 |
| RL-7 | RLRKRLRKFRRK | 1713.16 | 1712.80 | +10 | 16.2 | >50 |
| RL-8 | GLRKLLRKFLNK | 1485.89 | 1485.29 | +6 | 31.5 | 50 |
| RL-9 | GLRKLLRKFRRK | 1571.00 | 1570.40 | +8 | 19.5 | >50 |
| RL-10 | GLRKRLRKFLRK | 1571.00 | 1570.45 | +8 | 26.8 | >50 |
| RL-11 | RLRKLLRKFLNK | 1585.02 | 1584.49 | +7 | 26.1 | >50 |
| RL-12 | RLRKLLRKFRRK | 1670.13 | 1669.56 | +9 | 17.1 | >50 |
| RL-13 | RLRKRLRKFLRK | 1670.13 | 1669.55 | +9 | 19.4 | >50 |
| RL-14 | GLRKLLRKFLRK | 1527.97 | 1527.43 | +7 | 29.7 | 30 |
| RL-15 | RLRKLLRKFLRK | 1627.11 | 1626.49 | +8 | 25.5 | 25 |

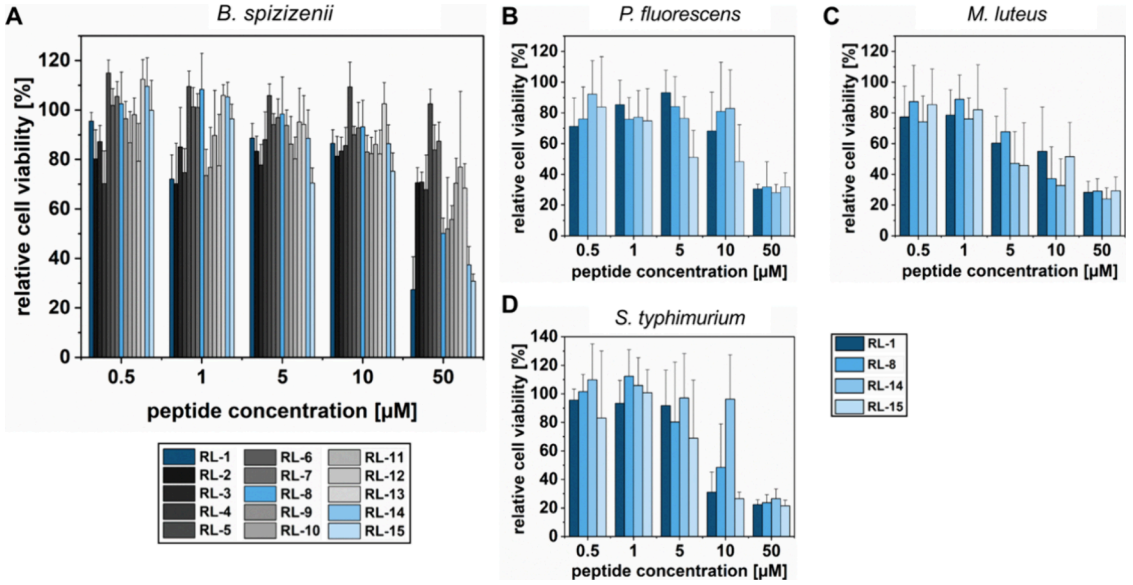


**Figure 1.** Screening the antimicrobial activity of the novel peptides against *B. spizizenii* (A), *P. fluorescens* (B), *M. luteus* (C), and *S. typhimurium* (D). For experiments (B–D), bacteria were incubated in minimal medium. Untreated bacteria served as negative control. The assays were conducted in triplicates ($n$ = 3). Values were normalized against the untreated control. Error bars represent standard deviations.

peptides.[18,19] In fact, both CPPs and AMPs share many physicochemical characteristics, letting us assume similar functionalities. Actually, CPPs have been developed as AMPs, and only recently, we have also demonstrated that transition of the CPP sC18 toward antimicrobial activity is possible.[20] Notably, in this work, we found that amphipathicity as well as the formation of a helical secondary structure are important key properties to enhance antimicrobial efficacy.

Herein, we aimed to further improve the antimicrobial properties of a shorter variant of sC18, namely, sC18*, lacking the last four N-terminal amino acids. In a recent study, we have created the peptide variant $sC18^{*R,L}$ including leucine and arginine substitutions to generate a nearly "perfect" amphipathic helix.[15] Essentially, this peptide was characterized by high membrane activity against cancerous cells. Encouraged by this observation, we hypothesized also antibacterial activity for this peptide and wanted to further elaborate the relevance of an amphipathic helical structure as a key property for membrane activity. Therefore, we rationally designed several additional variants of sC18* by amino acid substitution and screened for their antimicrobial activity. The most active sequence was then optimized by introducing a triazole-bridge with the goal to provide prestructured peptides with an optimized membrane interaction. Indeed, the triazole-bridged peptides exhibited far higher antimicrobial activities compared to the linear ones, even against pathogenic bacterial strains, such as *Neisseria gonorrhoeae* and methicillin-resistant *S. aureus*. Strikingly, we also measured high cytotoxicity caused by the membrane disturbing effects against human cancer cells. Since the novel peptides did not indicate prominent toxicity against human blood cells and exhibited good stability against enzymatic degradation, they might count as promising novel alternatives for future investigations.

## RESULTS AND DISCUSSION

**Design of R,L-sC18* Variants and Their Biological Screening.** We used the shorter variant sC18* (GLRKRLRK-FRNK) as a starting point and substituted different positions,


https://doi.org/10.1021/acsinfecdis.4c00078
ACS Infect. Dis. XXXX, XXX, XXX−XXX

e.g., 1, 4, 10, and 11, either with leucine or arginine to generate amphipathic peptides having differently balanced hydrophobic and hydrophilic parts (see helical wheel projections in Figure S1).[21] Furthermore, we introduced one to four replacements at the same time into the peptide sequence yielding peptides RL-1 to RL-15, respectively (Table 1). All peptides were synthesized by automated solid-phase peptide synthesis (SPPS) on a Rink amide resin.

First, we screened all peptides against Gram-positive *Bacillus spizizenii*[22] by incubating bacteria for 4 h with several concentrations of the distinct peptides. Within this first screen, we identified peptides RL-1, RL-8, RL-14, and RL-15 as the most active ones (Table 1 and Figure 1A). Interestingly, although RL-7 contains the highest net charge, it did not exhibit one of the highest activities measured. RL-7 comprises a large basic face and a relatively small hydrophobic one (three amino acids), letting one conclude that charge alone is not the only determinant for antimicrobial activity but that amphipathicity and hydrophobic content are probably more important. Maybe this was the reason that also other variants exhibited only minor cytotoxic effects or were not harmful at all, even when tested at 50 $\mu$M concentrations (e.g., RL-5, -6 and RL-11, -12). Actually, RL-1, which also contains a large basic face similar to RL-7, displayed significantly higher activity than RL-7. RL-1 still bears asparagine in the basic region, and it has been recently demonstrated that interhelix hydrogen bonding involving asparagine might drive di- or trimerization of transmembrane helices.[23] In fact, it is well established that hydrogen bonding between polar residues such as Asn−Asn pairing can drive helix−helix interactions and promote helical hairpins during membrane protein assembly or coiled−coiled formation.[24] Therefore, it might be that the asparagine present in the sequence of RL-7 (and similar variants) is responsible for the formation and stabilization of the peptide transmembrane assembly and hence is a key player for the observed antimicrobial activity. Another important characteristic for activity was attributed to the presence of relatively balanced hydrophobic/hydrophilic parts within the helix, which is the case for RL-8, RL-14, and RL-15.

Therefore, we selected the four peptides RL-1, RL-8, RL-14, and RL-15 for further studies and tested them against other bacterial strains including Gram-negative *Salmonella typhimurium* and *Pseudomonas fluorescens* and Gram-positive *Micrococcus luteus*, since each strain may be seen as representative of similar pathogenic species. Previously, it has been discussed that growth media can affect the strength of minimal inhibitory concentrations.[25] We also observed that $EC_{50}$ values varied between our performed studies, making interpretation of the data difficult. Beside other factors, a significant effect that influences bacterial growth might be the used growth medium composition.[26] Therefore, in our next experiments, bacteria were grown in normal cell culture medium, but to determine the $EC_{50}$ values, they were supplemented with minimal medium ($H_2O$, 5 mM glucose, 10 mM Tris) and incubated for 4 h with different peptide concentrations (Figure 1B−D; for *B. spizizenii*, see Figure S2). The activity against Gram-positive bacteria *B. spizizenii* and *M. luteus* was not significantly different between the various RL-peptides. On the other side, RL-14 demonstrated the lowest activity against Gram-negative *S. typhimurium*, while RL-1, RL-8, and RL-14 exhibited nearly the same activity. *P. fluorescens* was most affected by RL-14, while the other peptides showed similar activities. However, in all experiments, we observed that bacteria were dead at the highest concentration tested (50 $\mu$M) (see Table 2).

**Table 2. Half Maximal Effective Concentration, $EC_{50}$ [$\mu$M], of Peptides RL-1, -8, -14, and -15 against *M. luteus*, *S. typhimurium*, and *P. fluorescens***

| | $EC_{50}$ [$\mu$M] | | |
|---|---|---|---|
| Peptide | *M. luteus* | *S. typhimurium* | *P. fluorescens* |
| RL-1 | 15 | 7.5 | 20 |
| RL-8 | 7.5 | 10 | 25 |
| RL-14 | 5 | 25 | 25 |
| RL-15 | 10 | 7.5 | 10 |

**Triazole-Bridged Peptides and Their Secondary Structures.** Our results thus far let us conclude that the formation of an amphipathic helix acts as a driving force and is a key factor for the observed antimicrobial activity. Thus, we hypothesized that a preformed helical structure by side-chain to side-chain cyclization would cause enhanced membrane interaction and antimicrobial activity. In previous studies, we successfully introduced triazole-bridges for rigidification of the peptide backbone; wherefore, we used this strategy also in this work.[16,27] In addition, we chose RL-8 for the next experiments since it was demonstrated to be promising in all assays and still contained the asparagine in its hydrophilic part of the helix that we assumed to be important for membrane insertion and stabilization of the helix.

We designed four different peptides having triazole bridges either in the basic/hydrophilic or in the hydrophobic part (Figure 2). Synthesis was achieved by introducing Fmoc-propargylglycine-OH (Pra) and Fmoc-azidolysine-OH (Aza) at positions 4 and 8 of RL-8 (and *vice versa*) to obtain peptides 8A and 8B, respectively. Peptides 8C and 8D were obtained by replacing positions 2 and 6 with the respective building blocks. Thus, the triazolyl moiety is flanked by a total of 5 methylenes, which has been previously reported to be the optimal length to stabilize the $\alpha$-helical structure.[28] We changed the positions of Pra and Aza to find out how the different arrangements of the triazole-bridge would eventually influence secondary structure formation and, thus, biological activity. Synthesis of the peptides was performed on Tentagel resin, and the triazole was generated by Cu(I)-catalyzed azide−alkyne cycloaddition (CuAAC), the so-called click reaction introduced for the first time in peptides by the 2022 Nobel Prize in Chemistry by Morten Meldal.[29] Side-chain to side-chain triazolyl bridge formation was performed on the solid support using microwave irradiation, as we previously reported (see Table 3 and Figures S3−S6).[30]

Then, we investigated the secondary structures of the novel side-chain to side-chain triazolyl bridged peptides and performed CD spectroscopy in phosphate buffer and phosphate buffer with the addition of 25% trifluoroethanol (TFE). As shown in Figure 3, the linear peptide analogue RL-8 was unstructured when solved in aqueous solution, but it adopted an alpha helical structure when the biomimetic TFE solvent was added. This observation was somehow expected and also in line with our previous results on the secondary structure formation of sC18 and other sC18-related peptides.[15,20] More interesting was that all of the cyclopeptides, 8A-D, adopted a helical structure already in phosphate buffer, and this was even more pronounced when 25% TFE was added.


https://doi.org/10.1021/acsinfecdis.4c00078
ACS Infect. Dis. XXXX, XXX, XXX−XXX

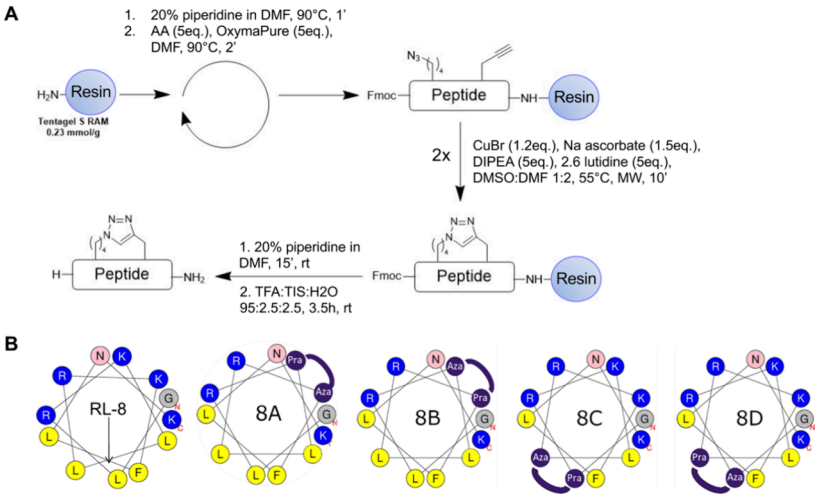


**Figure 2.** (A) General synthetic scheme to yield triazole-bridged RL-peptides. (B) Helical wheel projections showing the location of the triazole within the peptides. Aza: azidolysine; Pra: propargylglycine.

**Table 3. Names, Amino Acid Sequences, Molecular Weights (MWs), Net Charges, and Hydrophobicity as Measured by HPLC of All Triazole-Bridged Peptides**

| Name | Sequence | $MW_{calc.}$ [Da] | $MW_{exp.}$ [Da] | Net charge | Hydrophobicity |
|---|---|---|---|---|---|
| 8A | 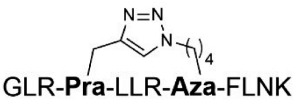 GLR-**Pra**-LLR-**Aza**-FLNK | 1478.8 | 1478.2 | +4 | 42.5 |
| 8B | 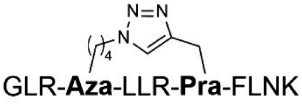 GLR-**Aza**-LLR-**Pra**-FLNK | 1478.8 | 1478.2 | +4 | 41.8 |
| 8C | 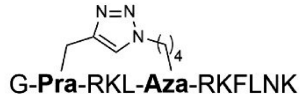 G-**Pra**-RKL-**Aza**-RKFLNK | 1508.8 | 1508.2 | +6 | 21.5 |
| 8D | 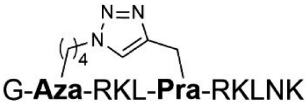 G-**Aza**-RKL-**Pra**-RKLNK | 1508.8 | 1508.2 | +6 | 19.3 |

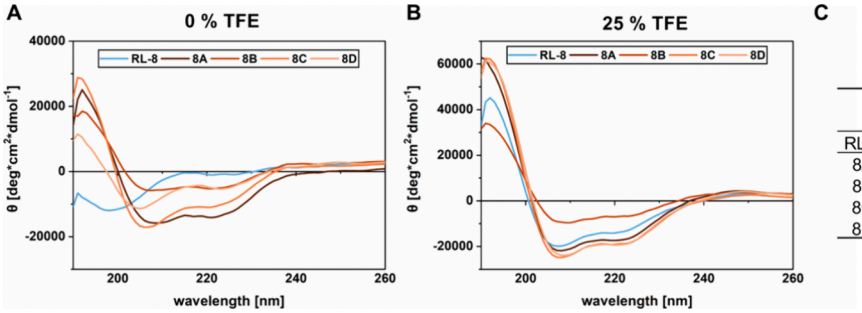


**Figure 3.** CD spectra of triazole-bridged RL-peptides in either phosphate buffer (A) or phosphate buffer with 25% TFE (B). (C) Summarizes the content of helicity expressed as *R*-values (calculated as the ratio between the minima measured at 220 and 208 nm).

In addition, calculating the fraction of helicity for each peptide substantiated the improved $\alpha$-helical formation for the triazole-bridged peptides compared to their linear version.[31] Since recent work documented that a preformed helical



https://doi.org/10.1021/acsinfecdis.4c00078
ACS Infect. Dis. XXXX, XXX, XXX−XXX

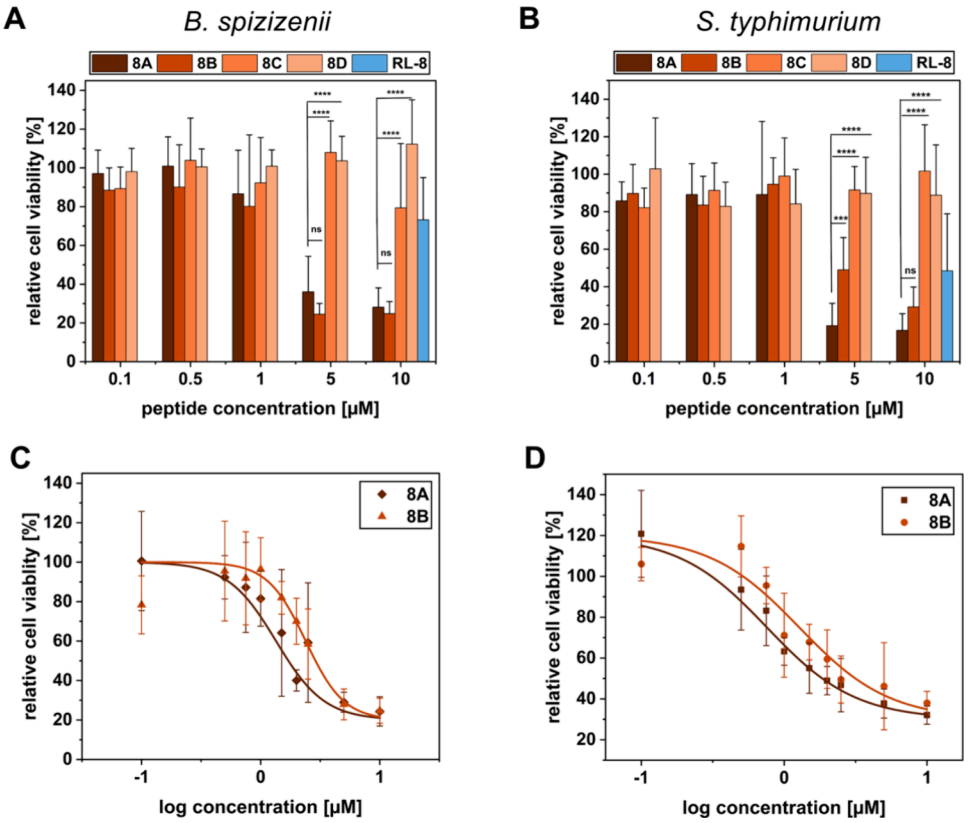


**Figure 4.** Activity assays of novel triazolyl bridged peptides 8A−D against *B. spizizenii* (A) and *S. typhimurium* (B). Bacteria were treated with the respective peptide concentrations for 4 h. Untreated cells served as negative control. (C, D) Results of the dose−response assay using *B. spizizenii* (C) and *S. typhimurium* (D) (see Methods). Assays were conducted in triplicates ($n$ = 3). Values were normalized against the untreated control. Error bars represent standard deviation. Statistical analyses were performed using one-way ANOVA test (****$p$ < 0.00001, ns $p$ > 0.05).

secondary structure promotes peptide−lipid interaction,[32] we assumed improved membrane insertion and hence efficacy of the newly designed peptides.

**Antimicrobial Activity and Membrane Interaction.** For proving our hypothesis, we first tested them in *B. spizizenii* and *S. typhimurium*, and indeed, we assessed markedly higher activities for the two triazolyl bridged peptides 8A/B compared to the linear version RL-8, while 8C/D exhibited fewer toxic effects (Figure 4A,B). This clear difference between 8A/B and 8C/D peptides was probably related to the different localizations of the triazole-bridge within the peptide backbone (Figure 2B). Actually, antibacterial activity was strongly enhanced when the triazole bridge was placed in the hydrophilic part, as was the case with 8A/B. On the other side, cyclopeptides 8C/D were significantly less effective, showing no activity at all at the highest concentration tested in both strains (10 $\mu$M). Moreover, we assumed slightly better activity for 8A compared to 8B in this assay. Thus, we recorded dose−response curves for both peptides in the same bacterial strains and indeed measured prominently lower $EC_{50}$ values for 8A compared to 8B (Figure 4C,D and Table 4).

To get some more insight into the activity mechanism of the peptides against *B. spizizenii* and *S. typhimurium*, we performed transmission electron microscopy (TEM) studies. We decided to compare the linear RL-8 peptide with the most potent triazole-bridged peptide, 8A. After 4 h of incubation with the peptides, we looked for intracellular changes and observed mainly dead cells in both treated strains (Figure 5). Obviously, the peptides had a strong impact on membrane integrity leading to disrupted outer membranes and/or pore formation

**Table 4. Half Maximal Effective Concentration, $EC_{50}$ [$\mu$M], of Triazolyl Bridged Peptides 8A−D against *B. spizizenii* and *S. typhimurium***

| | $EC_{50}$ [$\mu$M] | |
|---|---|---|
| Peptide | *B. spizizenii* | *S. typhimurium* |
| 8A | 1.35 ± 0.12 | 0.75 ± 0.09 |
| 8B | 2.39 ± 0.20 | 1.28 ± 0.12 |
| 8C | >10 | >10 |
| 8D | >10 | >10 |

that resulted in an outflow of intracellular material. In addition, the higher activity of 8A compared to the linear RL-8 was impressively visible after incubation with *B. spizizenii* since, here, the shape of the cells was nearly completely destroyed. Also, after treatment of *S. typhimurium* with 8A, only few viable cells were counted, and many cells developed large intracellular empty spaces and showed blebbing. All in all, the images provided further proof for the membrane permeabilizing effects of the triazole-bridged peptides and, thus, further confirmed their high membrane activity.

**Exploring Activity against Pathogenic Bacterial Species.** Since cyclopeptides 8A/B proved to be more effective than 8C/D, we proceeded with all further studies using only these variants. Encouraged by the former results, we examined peptides 8A/B against two pathogenic strains, namely, Gram-negative *N. gonorrhoeae* and Gram-positive methicillin-resistant *S. aureus* (MRSA). Slightly different $EC_{50}$ values were detected in *N. gonorrhoeae* for 8A compared to 8B, but both were again significantly more active than the linear


https://doi.org/10.1021/acsinfecdis.4c00078
ACS Infect. Dis. XXXX, XXX, XXX−XXX

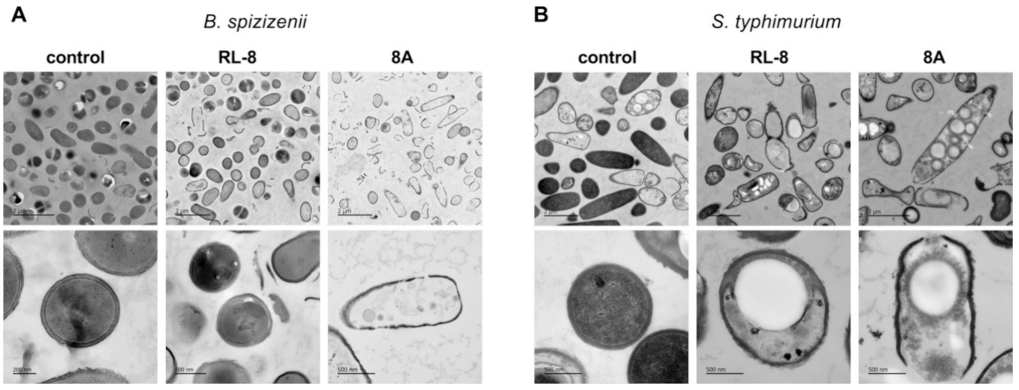


**Figure 5.** Transmission Electron Microscopy (TEM) pictures of *B. spizizenii* (A) and *S. typhimurium* (B) after treating bacteria for 4 h with 5 $\mu$M of each peptide. Each condition was captured zoomed out at 5,000× (upper row) and zoomed in at 25,000−40,000× (lower row).

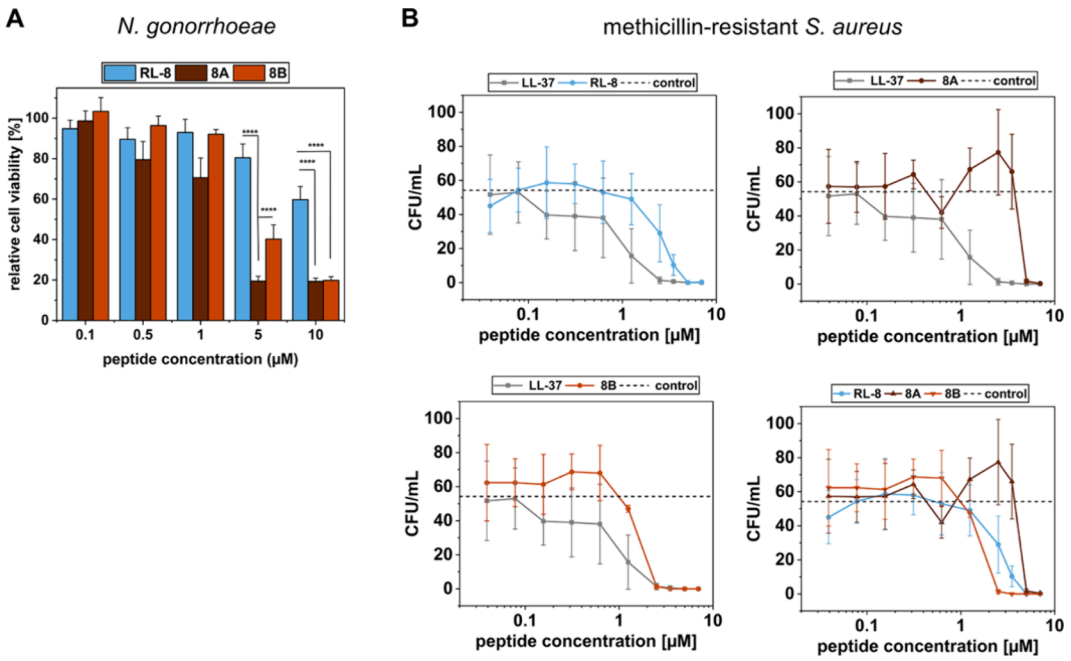


**Figure 6.** Activity assays against *N. gonorrhoeae* (A) and methicillin-resistant *S. aureus* (B). Assays were conducted in triplicates ($n$ = 3). Values were normalized against the untreated control. Error bars represent standard deviation. Statistical analyses were performed using a one-way ANOVA test (****$p$ < 0.00001, ***$p$ < 0.0001, ns $p$ > 0.05).

version (Figure 6A). This observation was somehow reversed upon examination of the peptides against the MRSA strain (Figure 6B). Interestingly, the linear RL-8 peptide was capable of reducing the number of counted colonies nearly as efficiently as 8B, while 8A did not maintain its previously demonstrated highest activity. Also, all peptides were slightly less powerful than the control AMP LL-37, which has been used in many (pre)clinical studies to address bacterial, fungal, or viral infections.[33] Although the assays used to determine the $EC_{50}$ values were different and thus not directly comparable, we assume a slightly higher activity of peptides 8A/B against the herein tested Gram-negative bacteria (*S. typhimurium* and *N. gonorrhoeae*) compared to Gram-positive bacteria (*B. spizizenii* and MRSA *S. aureus*). This might be related to a less well integration of 8A/B into the peptidoglycan layer of Gram-positive bacteria. On the other hand, Gram-negative bacteria possess a second outer membrane to which 8A/B might be highly attracted. Moreover, the presence of lipopolysaccharides might also induce a first binding and interaction of the peptides with the outer surface of the bacteria. Notably, when testing the activity against *P. aeruginosa*, all tested peptides, the linear RL-8 as well as the triazolyl-bridged peptides 8A/B, were only less active (data not shown). Maybe this observation is due to different interactions of the peptides with bacterial surface components, a matter that we investigate in ongoing studies.

**Stability in Blood Serum and Cytotoxicity of Peptides to Mammalian Cells.** Next, we assessed the proteolytic stability of peptides 8A/B when in contact with blood serum proteins since it has been found before that cyclopeptides show increased stability toward degradation by proteases.[34] In addition, the presence of the triazole-bridge might lead to higher resistance against enzymatic cleavage, an effect that we previously observed for similar peptides.[16] 8A/B and the linear RL-8 as control were treated for 240 min in goat serum, and samples were analyzed at several time points using LC-MS (Figure 7). After only 60 min incubation time, the linear peptide RL-8 was no longer detectable in the sample solution. Contrarily, both triazole-bridged peptides demonstrated prolonged serum stability with almost or even more than 50% of the compounds still intact after 120 min and up to 240


https://doi.org/10.1021/acsinfecdis.4c00078
ACS Infect. Dis. XXXX, XXX, XXX−XXX

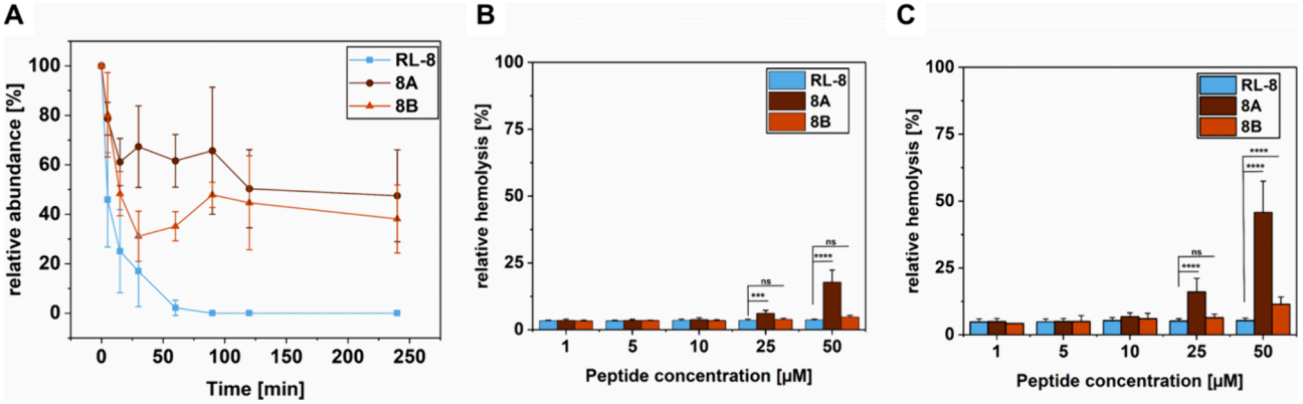


**Figure 7.** (A) Analysis of peptide stability in the presence of goat serum. Peptides were incubated for 240 min, and samples were taken at respective time points and precipitated in acetonitrile. Peptide abundance was measured using LC-MS and normalized to time point zero. (B, C) Hemolytic activity in the presence of human red blood cells (RBCs). RBCs were diluted 1:20 in PBS and treated for (B) 30 min or (C) 24 h with 1, 5, 10, 25, or 50 $\mu$M peptide solutions. RBCs treated with PBS only served as negative control, whereas cells treated with Triton-X-100 indicated 100% hemolysis. All experiments were performed in triplicates ($n$ = 3). Statistical analyses were performed using a one-way ANOVA test (****$p$ < 0.00001, ***$p$ < 0.0001, ns $p$ > 0.05).

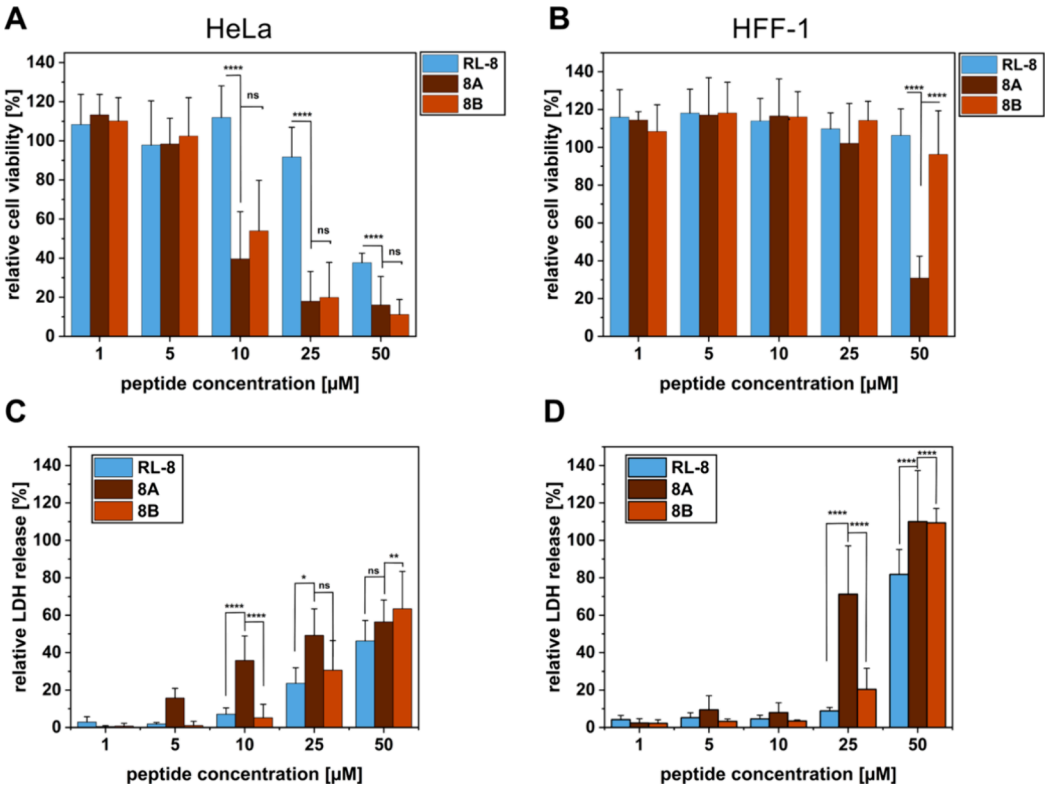


**Figure 8.** Cell viability assays using HeLa (A, C) and HFF-1 (B, D) cells. In (A) and (B), a resazurin-based cell-proliferation assay was performed and cells were incubated for 24 h at the indicated concentrations. (C) and (D) display the results of an LDH release assay, in which cells were treated for 30 min with different peptide concentrations before measuring LDH release. All assays were conducted in triplicates ($n$ = 3). Values were normalized against the untreated control. Error bars represent standard deviation. Statistical analyses were performed using a one-way ANOVA test (****$p$ < 0.00001, ***$p$ < 0.0001, **$p$ < 0.001, *$p$ < 0.05, ns $p$ > 0.05).

min. Probably, this was a result of complex formation between 8/B and serum proteins such as BSA, which we identified in all samples. Owing to its negative charges, BSA might easily interact with the positively charged peptides.

Furthermore, we investigated the hemolytic activity of triazole-bridged peptides 8A/B compared to RL-8 when in contact with human red blood cells (RBCs). Therefore, we measured the hemoglobin release after 30 min or 24 h, respectively. Interestingly, for all samples tested, we observed negligible hemoglobin release (<20%) when RBCs were incubated for 30 min with different peptide concentrations. However, after 24 h of incubation with 8A, a clear release of hemoglobin was measured pointing to cytotoxic and more specifically membrane-active effects of 8A. This would agree with the general membrane disturbing effects that we had observed in the TEM studies before. Of note was that 8B did not show this significantly increased release, suggesting that this peptide is less membrane active. Moreover, our findings


https://doi.org/10.1021/acsinfecdis.4c00078
ACS Infect. Dis. XXXX, XXX, XXX−XXX

might be explained by the different membrane compositions of bacterial cells compared to RBCs. Usually, bacterial membranes contain more negatively charged components at the outer surface, such as, for instance, phosphatidylserine. In contrast, the outer membrane layer of human erythrocytes is mainly composed of neutrally charged phospholipids.[30,31] Since the peptides have a positive net charge, they favorably interact with the more negatively charged membranes of bacteria. Hence, our observations also hint at higher selectivity against bacterial cells compared to, for example, RBCs and probably also to other human cells.

**Activity against Human Cancer and Noncancer Cells.** To test our hypothesis, we explored the activity of RL-8, -8A, and -8B against different human cell lines including cancerous and noncancerous cells. During recent years, AMPs were elaborated as anticancer peptides (ACPs) in various types of cancer.[35] ACPs act by similar processes against cancer cells and most often disturb the structure of the phospholipid bilayer and form pores leading to cell lysis.[36]

In previous studies, we have already observed such effects for several sC18 variants[15,20] and, thus, elucidated the activity of the triazole-bridged peptides when in contact with cancerous HeLa cells. After incubating the cells for 24 h with various peptide concentrations, we found the highest toxicity for peptides 8A and 8B, demonstrating again their increased activity compared to the linear RL-8. Peptide-induced cell toxicity was also tested against noncancerous human foreskin fibroblast (HFF-1) cells. All peptides showed no or negligible toxicity until the highest concentration tested, beside 8A that caused toxicity at 50 $\mu$M. Yet, 8A was not toxic at lower concentrations at which this peptide was active against the pathogenic bacteria (Figure 8B).

To get a more detailed view on the mechanism of action, we conducted a lactate dehydrogenase (LDH) release assay, which provides information about membrane lytic effects of the peptides. After 30 min of peptide incubation, the strongest effects were measured for 8A that impaired HeLa cell membrane integrity already at a 5 $\mu$M concentration. However, at 25 $\mu$M, also 8B and the linear RL-8 peptide provoked LDH release in HeLa cells, which was even increased at 50 $\mu$M, and pointed to clear membranolytic effects toward this cell line for all peptides investigated (Figure 8C). Also, this finding supports the results of the cell proliferation assay in this cell line. However, HFF-1 cells were not harmed at lower concentrations, while at 25 $\mu$M, 8A incubation yielded significant LDH release. Remarkably, in HFF-1 cells, all peptides induced complete LDH release at the highest concentration tested (50 $\mu$M) compared to HeLa cells, where only around 40−60% LDH release was measured at this concentration. Since we did not observe cytotoxic effects after longer incubation times for peptides RL-8 and 8B, we concluded that these peptides possess indeed a strong membrane activity, but cells can recover over time. 8A might act mainly by perturbating the membrane and pore formation, leading to cell lysis. In conclusion, in HFF-1 cells, 8A demonstrated the highest membrane activity but not at the same concentrations where it exhibited antimicrobial activity. Thus, they are still valuable for further therapeutic application. Moreover, since 8A indicated cytotoxic effects toward cancer cells, it is also an attractive candidate to develop further as an anticancer peptide.

## CONCLUSION

Upcoming antibiotic resistance is still a major burden, and it has been predicted that bacterial infections will be responsible for increasing death rates worldwide. Therefore, it is highly important to find and develop new drugs to face the developing high number of multiple resistant bacterial strains. Herein, we propose novel antimicrobial peptides that were stapled by a triazole-bridge to support alpha helical formation, one major characteristic for the interaction and activity of antimicrobial peptides with bacterial membranes. One of these novel peptides, namely, 8A, exhibited highly promising antibacterial activity, also toward pathogenic bacterial species such as *N. gonorrhoeae* and MRSA. We also found that 8A is stabilized against proteolytic cleavage and that it exhibits higher selectivity against bacteria compared to human red blood and fibroblast cells. Additionally, cytotoxic effects against cancer cells were detected, making 8A an interesting and promising candidate to explore in various biological settings.

## METHODS

**Materials.** N$\alpha$-Fmoc protected amino acids were purchased from IRIS Biotech (Marktredwitz, Germany). Other chemicals and consumables including 1-[bis(dimethylamin)methylen]-1*H*-1,2,3-triazol[4,5-*b*]pyridinium-3-oxide hexafluorophosphate (HATU), *N*,*N*-diisopropylethylamine (DIPEA), acetonitrile (ACN), trifluoroacetic acid (TFA), doxorubicin hydrochloride (Dox), *N*-succinimidyl-3-maleimidopropionate (SMP), *N*,*N*′-diisopropylcarbodiimide (DIC), triethanolamine (TEA), and 5(6)-carboxyfluorescein (CF) were derived from Fluka (Taufkirchen, Germany), Merck (Darmstadt, Germany), Sarstedt (Nümbrecht, Germany), Sigma-Aldrich (Taufkirchen, Germany), and VWR (Darmstadt, Germany).

The bacterial strains used include: *Bacillus spizizenii* (ATTC 6633, *Bacillus spizizenii* subsp. *spizizenii*, which has similar morphological, physiological, and biochemical characteristics as *Bacillus subtilis* subsp. *subtilis*,[37] was recently promoted to full species by Dunlap et al.[22]), *Micrococcus luteus* (DSM 20030), *Salmonella typhimurium* (TA 100), *Pseudomonas fluorescens* (DSM 50090), methicillin resistant *Staphylococcus aureus* (MRSA-43300), and *Neisseria gonorrhoeae* Ng196 (*pilE::cat, G4::acc*).[38]

**Solid Phase Peptide Synthesis.** All peptides were synthesized on Rink amide resin by automated SPPS on a multiple Syro II peptide synthesizer (MultiSyntech, Witten, Germany) following the Fmoc/tBu-strategy as recently described. Briefly, amino acids were coupled using a double-coupling procedure and in situ activation with Oxyma/DIC according to recent work.[15] Purification of peptides was achieved by preparative reverse phase HPLC on a C18 column and analyzed analytically by HPLC ESI-MS (LTQ XL, Thermo Scientific, Waltham, MA, USA). Purified peptides were evaporated and lyophilized with purities >97%.

**Synthesis of Triazole-Bridged Peptides.** All cyclopeptides 8A−8D were synthesized on Tentagel S RAM resin by automated High Efficiency Solid Phase Peptide synthesis (HE-SPPS) on the microwave-assisted Liberty Blue 2.0 peptide synthesizer (CEM, Charlottesville, VA, U.S.A.) following the Fmoc/tBu-strategy. After HE-SPPS of the linear precursor, the click reaction was performed. Therefore, peptides were treated two times with 1.2 equiv. of CuBr, 1.5 equiv. of sodium ascorbate, 5 equiv. of DIPEA, and 5 equiv. of 2.6 lutidine in DMS:DMF (1:2, v/v) at 55 °C. Purification of


https://doi.org/10.1021/acsinfecdis.4c00078
ACS Infect. Dis. XXXX, XXX, XXX−XXX

the peptides was performed by RP-HPLC on an Alliance Chromatography equipped with a BEH C18 column. Peptides were analyzed by analytical ESI-MS (Single Quadrupole ESI-MS Micro mass ZQ; Waters, Milford Massachusetts, U.S.A.).

**Circular Dichroism (CD) Spectroscopy.** CD spectra were recorded using a JASCO J-715 spectropolarimeter (JASCO, Pfungstadt, Germany) under a $N_2$ atmosphere. The CD spectra were measured from 180 to 270 nm in 1 nm intervals at 20 °C using a 1 mm quartz cuvette, and the instrument parameters were set as follows: sensitivity, 100 mdeg; scan mode, continuous; scan speed, 50 nm/min; response time, 2 s; bandwidth, 2.0 nm; 20 $\mu$M peptide solutions in 10 mM potassium phosphate buffer (pH 7.0) were inspected containing either 0 or 25% (v/v) trifluoroethanol (TFE).

**Antimicrobial Activity Assay.** Bacterial cultures with an optical density of more than 0.7 at 600 nm were used. In a 96-well plate, 180 $\mu$L of minimal medium (10 mM Tris, 5 mM glucose) and for *N. gonorrhoeae* (Gonococcal (GC)) liquid medium was made from 5 g/L NaCl (Roth), 4 g/L $K_2HPO_4$ (Roth), 1 g/L $KH_2PO_4$ (Roth), and 15 g/L Proteose Peptone No. 3 (BD Biosciences), supplemented with 1% IsoVitaleX (IVX). IVX was made from 1 g/L D-glucose (Roth), 0.1 g/L L-glutamine (Roth), 0.289 g/L L-cysteine-HCL·$H_2O$ (Roth), 1 mg/L thiamine pyrophosphate (Sigma-Aldrich), 0.2 mg/L $Fe(NO_3)_3$ (Sigma-Aldrich), 0.03 mg/L thiamine HCL (Roth), 0.13 mg/L 4-aminobenzoic acid (Sigma-Aldrich), 2.5 mg/L $\beta$-nicotinamide adenine dinucleotide (Roth), and 0.1 mg/L vitamin B12 (Sigma-Aldrich). A 10 $\mu$L portion of bacteria suspension and 10 $\mu$L of peptide solution were mixed. The resulting cultures were screened at several different peptide concentrations (as triplicates). Pure water was the negative control, and antibiotics were used as positive controls. All samples were then incubated at 37 °C for 4 h. Afterward, 10 $\mu$L of a 1 mg/mL solution of iodonitrotetrazolium chloride in pure DMSO was added to each well, and samples were further incubated for 15 min at 37 °C. Finally, the absorption of formazan at 560 nm in each well was measured using a Tecan infinite M200 plate reader (Tecan Group AG, Männedorf, Switzerland). To calculate the $EC_{50}$ value of the used peptides, a sigmoidal fit was calculated by fitting with the dose response function of the computational program Origin. The fit of the graph is used for the following calculation:

$$EC_{50} = 10^{LOGx0}$$

The $x$ values are supposed to be the logarithm of dose; thereby, LOG$x$0 is the center of the curve, meaning the $EC_{50}$. The experiment was performed in three independent experiments in triplicate.

**Viable Count Assay.** Methicillin resistant *Staphylococcus aureus* (MRSA-43300) were cultivated in tryptic soy broth. The cells were counted at an OD of 620 nm. Bacteria were mixed with PG buffer (18.4 mM $K_2HPO_4$, 5 mM glucose, pH 7.4) and afterward centrifuged and resuspended after discarding the supernatant again with 1 mL of PG buffer. The bacterial culture was diluted again 1:10 and, afterward, 500 $\mu$L of this dilution was mixed with 4.5 mL of PG buffer. Each well was prefilled with 50 $\mu$L of PG buffer. Peptides were mixed directly in each well, and afterward, 50 $\mu$L of bacterial solution was added; the plate was incubated for 2 h at 37 °C. Bacterial cells were then diluted 1:10 and suspended 1:8 in PG buffer. 50 $\mu$L of diluted solution was plated into prewarmed TSB agar plates and incubated overnight at 37 °C. On the next day, colonies were counted.

**Cell Culture.** Cell lines HFF-1 (human foreskin fibroblasts, ATCC) as well as HeLa (human cervix carcinoma, ACC57) were used. HeLa cells were cultured in dishes containing RPMI-1640 (R0883) medium supplemented with 4 mM L-glutamine and 10% FBS. HFF-1 cells were cultured in flasks containing DMEM (D5030) medium supplemented with 4 mM L-glutamine and 10% FBS.

**Cytotoxicity Assay.** For cell viability assay, cells (15,000 HeLa and 12,000 HFF-1 cells per well) were seeded onto a 96-well plate and grown to 80−90% confluency. Cells were incubated with different peptide concentrations in a serum-free growth medium for 24 h under standard growth conditions. For the positive control, cells were treated with 70% EtOH for 7 min. After washing with DPBS, cells were treated with resazurin solution (10% in serum-free media, v/v) and incubated for 1 h under standard growth conditions. Cell viability was determined relative to untreated cells by measurement of the resorufin product at 595 nm ($\lambda_{ex}$ = 550 nm) on a Tecan infinite M200 plate reader (Tecan Group AG, Männedorf, Switzerland).

**Lactate Dehydrogenase Release Assay.** We used the CytoTox-One Homogeneous Membrane Integrity Assay by Promega for this experiment. 17,000 HeLa cells were seeded on a dark 96 well plate and grown to 80% confluency. Then, cells were treated with 100 $\mu$L peptide solutions at different concentrations and further incubated for 30 min. Afterward, the plate was equilibrated at room temperature for 20 min, and lysis buffer was added to obtain positive controls. Each well was then supplemented with the CytoTox-One reagent, and fluorescence was measured using a microtiter plate reader (excitation: 560 nm; emission: 590 nm).

**Transmission Electron Microscopy.** For transmission electron microscopy (TEM), bacterial cells were grown to an optical density of 1.0. A mixture of 100 $\mu$L of bacteria, 490 $\mu$L of minimal medium (10 mM Tris, 5 mM glucose), and 10 $\mu$L of peptide solution to reach a final concentration of 5 $\mu$M was prepared. Subsequently, all samples were incubated at 37 °C for 4 h while shaking. After incubation, the cells were pelleted at 10,000$g$. Supernatant was discarded, and pellet was dissolved in 1 mL of fixative (20 mM Hepes, 0.2 M Tris, 3% glutaraldehyde). Bacteria were immersion fixed in 2% glutaraldehyde, 2.5% sucrose, and 3 mM $CaCl_2$ in 0.1 M HEPES buffer for 30 min at room temperature and 30 min at 4 °C. Samples were washed with 0.1 M sodium cacodylate buffer and centrifuged for 10 min at 1,000$g$. The supernatant was removed, and the pellets were mixed with 3% low melting agarose in 0.2 M sodium cacodylate buffer, incubated for 10 min at 37 °C, and hardened at 4 °C for 30 min. Pellets were cut in pieces of 1 $mm^3$ and washed four times for 15 min with 0.1 M sodium cacodylate buffer. Postfixation, 1% $OsO_4$ (Science Services), 1.25% sucrose, and 1% potassium ferricyanide in 0.1 M sodium cacodylate buffer was applied for 2 h at 4 °C. Samples were washed four times with 0.1 M sodium cacodylate buffer and dehydrated using an ascending ethanol series (50%, 70%, 90%, 3 × 100%) for 15 min each. The sample was incubated with a mix of 50% ethanol/propylenoxide and two times with pure propylenoxide for 15 min for each step. Samples were infiltrated with a mixture of 50% Epon/propylenoxide and 75% Epon/propylenoxide for 2 h each at 4 °C and with pure Epon overnight at 4 °C. The next day, Epon was exchanged and samples were incubated for 2 h at room temperature. Samples were mounted onto Epon blocks and cured for 72 h at 60 °C.


https://doi.org/10.1021/acsinfecdis.4c00078
ACS Infect. Dis. XXXX, XXX, XXX−XXX

Ultrathin sections of 70 nm were cut using an ultramicrotome (Leica Microsystems, UC6) and a diamond knife (Diatome, Biel, Switzerland) and stained with 1.5% uranyl acetate for 15 min at 37 °C and 3% lead citrate solution for 4 min.

Images were acquired using a JEM-2100 Plus Transmission Electron Microscope (JEOL) operating at 80 kV equipped with a OneView 4K camera (Gatan).

**Statistical Analysis.** For experiments comparing data of two groups, a paired student *t* test was performed for statistical analysis using Microsoft Excel. Significances calculated by a paired student *t* test were defined as $*p < 0.05$, $**p < 0.005$, $***p < 0.0005$, and $****p < 0.00005$. For experiments comparing data from more than two groups, a one-way ANOVA was performed by using Microsoft Excel. Significances determined by one-way ANOVA were as follows: $*p < 0.05$, $**p < 0.01$, $***p < 0.001$, and $****p < 0.0001$.

## ■ ASSOCIATED CONTENT

### Supporting Information

The Supporting Information is available free of charge at https://pubs.acs.org/doi/10.1021/acsinfecdis.4c00078.

Helical wheel projections of peptides RL-1 to RL-15; INT assay of peptides when bacteria were placed in minimal medium; analytical data (chromatography and mass spectrometry) of peptides 8A−8D (PDF)

## ■ AUTHOR INFORMATION


### Corresponding Author

**Ines Neundorf** − *University of Cologne, Faculty of Mathematics and Natural Sciences, Department of Chemistry, Institute of Biochemistry, 50674 Cologne, Germany*; orcid.org/0000-0001-6450-3991; Email: ines.neundorf@uni-koeln.de

### Authors

**Joshua Grabeck** − *University of Cologne, Faculty of Mathematics and Natural Sciences, Department of Chemistry, Institute of Biochemistry, 50674 Cologne, Germany*

**Jacob Mayer** − *University of Cologne, Faculty of Mathematics and Natural Sciences, Department of Chemistry, Institute of Biochemistry, 50674 Cologne, Germany*

**Axel Miltz** − *University of Cologne, Faculty of Mathematics and Natural Sciences, Department of Chemistry, Institute of Biochemistry, 50674 Cologne, Germany*

**Michele Casoria** − *Interdepartmental Research Unit of Peptide and Protein Chemistry and Biology, Department of Chemistry "Ugo Schiff", University of Florence, 50019 Sesto Fiorentino, Italy*

**Michael Quagliata** − *Interdepartmental Research Unit of Peptide and Protein Chemistry and Biology, Department of Chemistry "Ugo Schiff", University of Florence, 50019 Sesto Fiorentino, Italy*; orcid.org/0000-0003-0891-3405

**Denise Meinberger** − *University of Cologne, Faculty of Medicine, Institute for Clinical Chemistry, 50937 Cologne, Germany*

**Andreas R. Klatt** − *University of Cologne, Faculty of Medicine, Institute for Clinical Chemistry, 50937 Cologne, Germany*

**Isabelle Wielert** − *University of Cologne, Faculty of Mathematics and Natural Sciences, Department of Physics, Institute for Biological Physics, 50674 Cologne, Germany*

**Berenike Maier** − *University of Cologne, Faculty of Mathematics and Natural Sciences, Department of Physics, Institute for Biological Physics, 50674 Cologne, Germany*

**Anna Maria Papini** − *Interdepartmental Research Unit of Peptide and Protein Chemistry and Biology, Department of Chemistry "Ugo Schiff", University of Florence, 50019 Sesto Fiorentino, Italy*; orcid.org/0000-0002-2947-7107

Complete contact information is available at: https://pubs.acs.org/10.1021/acsinfecdis.4c00078

### Author Contributions

†J.G. and J.M. contributed equally.


### Notes

The authors declare no competing financial interest.

## ■ ACKNOWLEDGMENTS

We thank the CECAD Imaging facility for their support (in TEM and data analysis). We thank Katharina Stillger for creative input and fruitful discussion. Financial support by EUniWell (5th Seed Funding Call) and the German Research Foundation (grant number NE14-10) are kindly acknowledged by I.N. Erasmus+ exchange program between University of Cologne and University of Florence is kindly acknowledged for M.C. fellowship. The PhD scholarship of M.Q. is funded by the "Progetto Ministeriale Dipartimenti di Eccellenza 2018-2022" (58503_DIPECC-C.U.P. B96C17000200008).

## ■ REFERENCES

(1) Hegemann, J. D.; Birkelbach, J.; Walesch, S.; Müller, R. Current Developments in Antibiotic Discovery. *EMBO Rep.* **2023**, *24* (1), e56184.

(2) Darby, E. M.; Trampari, E.; Siasat, P.; Gaya, M. S.; Alav, I.; Webber, M. A.; Blair, J. M. A. Molecular Mechanisms of Antibiotic Resistance Revisited. *Nat. Rev. Microbiol.* **2023**, *21* (5), 280−295.

(3) Yao, L.; Liu, Q.; Lei, Z.; Sun, T. Development and Challenges of Antimicrobial Peptide Delivery Strategies in Bacterial Therapy: A Review. *International Journal of Biological Macromolecules* **2023**, *253*, 126819.

(4) Mookherjee, N.; Anderson, M. A.; Haagsman, H. P.; Davidson, D. J. Antimicrobial Host Defence Peptides: Functions and Clinical Potential. *Nature Reviews Drug Discovery* **2020**, *19*, 311−332.

(5) Loffredo, M. R.; Nencioni, L.; Mangoni, M. L.; Casciaro, B. Antimicrobial Peptides for Novel Antiviral Strategies in the Current Post-COVID-19 Pandemic. *Journal of Peptide Science.* **2024**, *30*, e3534.

(6) Panjla, A.; Kaul, G.; Chopra, S.; Titz, A.; Verma, S. Short Peptides and Their Mimetics as Potent Antibacterial Agents and Antibiotic Adjuvants. *ACS Chem. Biol.* **2021**, *16* (12), 2731−2745.

(7) Omardien, S.; Drijfhout, J. W.; Vaz, F. M.; Wenzel, M.; Hamoen, L. W.; Zaat, S. A. J.; Brul, S. Bactericidal Activity of Amphipathic Cationic Antimicrobial Peptides Involves Altering the Membrane Fluidity When Interacting with the Phospholipid Bilayer. *Biochim. Biophys. Acta - Biomembr.* **2018**, *1860* (11), 2404−2415.

(8) Liang, Y.; Zhang, X.; Yuan, Y.; Bao, Y.; Xiong, M. Role and Modulation of the Secondary Structure of Antimicrobial Peptides to Improve Selectivity. *Biomater. Sci.* **2020**, *8* (24), 6858−6866.

(9) Cao, F.; Ma, G.; Song, M.; Zhu, G.; Mei, L.; Qin, Q. Evaluating the Effects of Hydrophobic and Cationic Residues on Antimicrobial Peptide Self-Assembly. *Soft Matter* **2021**, *17* (16), 4445−4451.

(10) Benfield, A. H.; Henriques, S. T. Mode-of-Action of Antimicrobial Peptides: Membrane Disruption vs. Intracellular Mechanisms. *Front. Med. Technol.* **2020**, *2*, 25−28.

(11) Wang, X.; Yang, X.; Wang, Q.; Meng, D. Unnatural Amino Acids: Promising Implications for the Development of New Antimicrobial Peptides. *Crit. Rev. Microbiol.* **2023**, *49* (2), 231−255.

(12) Chowdhary, R.; Mubarak, M. M.; Kantroo, H. A.; ur Rahim, J.; Malik, A.; Sarkar, A. R.; Bashir, G.; Ahmad, Z.; Rai, R. Synthesis, Characterization, and Antimicrobial Activity of Ultra-Short Cationic β-Peptides. *ACS Infect. Dis.* **2023**, *9* (7), 1437−1448.
(13) Shaikh, A. Y.; Björkling, F.; Zabicka, D.; Tomczak, M.; Urbas, M.; Domraceva, I.; Kreicberga, A.; Franzyk, H. Structure-Activity Study of Oncocin: On-Resin Guanidinylation and Incorporation of Homoarginine, 4-Hydroxyproline or 4,4-Difluoroproline Residues. *Bioorg. Chem.* **2023**, *141*, 106876.
(14) Derakhshankhah, H.; Jafari, S. Cell Penetrating Peptides: A Concise Review with Emphasis on Biomedical Applications. *Biomedicine and Pharmacotherapy* **2018**, *108*, 1090−1096.
(15) Grabeck, J.; Lützenburg, T.; Frommelt, P.; Neundorf, I. Comparing Variants of the Cell-Penetrating Peptide SC18 to Design Peptide-Drug Conjugates. *Molecules* **2022**, *27* (19), 6656.
(16) Reichart, F.; Horn, M.; Neundorf, I. Cyclization of a Cell-Penetrating Peptide via Click-Chemistry Increases Proteolytic Resistance and Improves Drug Delivery. *J. Pept. Sci.* **2016**, *22* (6), 421−426.
(17) Feni, L.; Parente, S.; Robert, C.; Gazzola, S.; Arosio, D.; Piarulli, U.; Neundorf, I. Kiss and Run: Promoting Effective and Targeted Cellular Uptake of a Drug Delivery Vehicle Composed of an Integrin-Targeting Diketopiperazine Peptidomimetic and a Cell-Penetrating Peptide. *Bioconjugate Chem.* **2019**, *30* (7), 2011−2022.
(18) Guha, S.; Ghimire, J.; Wu, E.; Wimley, W. C. Mechanistic Landscape of Membrane-Permeabilizing Peptides. *Chem. Rev.* **2019**, *119* (9), 6040−6085.
(19) Neundorf, I. *Antimicrobial and Cell-Penetrating Peptides: How to Understand Two Distinct Functions despite Similar Physicochemical Properties* **2019**, *1117*, 93.
(20) Drexelius, M.; Reinhardt, A.; Grabeck, J.; Cronenberg, T.; Nitsche, F.; Huesgen, P. F.; Maier, B.; Neundorf, I. Multistep Optimization of a Cell-Penetrating Peptide towards Its Antimicrobial Activity. *Biochem. J.* **2021**, *478* (1), 63−78.
(21) Gautier, R.; Douguet, D.; Antonny, B.; Drin, G. HELIQUEST: A Web Server to Screen Sequences with Specific α-Helical Properties. *Bioinformatics* **2008**, *24* (18), 2101−2102.
(22) Dunlap, C. A.; Bowman, M. J.; Zeigler, D. R. Promotion of Bacillus Subtilis Subsp. Inaquosorum, Bacillus Subtilis Subsp. Spizizenii and Bacillus Subtilis Subsp. Stercoris to Species Status. *Antonie van Leeuwenhoek, Int. J. Gen. Mol. Microbiol.* **2020**, *113* (1), 1−12.
(23) Hessa, T.; Kim, H.; Bihlmaier, K.; Lundin, C.; Boekel, J.; Andersson, H.; Nilsson, I. M.; White, S. H.; Von Heijne, G. Recognition of Transmembrane Helices by the Endoplasmic Reticulum Translocon. *Nature* **2005**, *433* (7024), 377−381.
(24) Thomas, F.; Niitsu, A.; Oregioni, A.; Bartlett, G. J.; Woolfson, D. N. Conformational Dynamics of Asparagine at Coiled-Coil Interfaces. *Biochemistry* **2017**, *56* (50), 6544−6554.
(25) Štumpf, S.; Hostnik, G.; Primožič, M.; Leitgeb, M.; Salminen, J. P.; Bren, U. The Effect of Growth Medium Strength on Minimum Inhibitory Concentrations of Tannins and Tannin Extracts against E. Coli. *Molecules* **2020**, *25* (12), 2947−2961.
(26) Balouiri, M.; Sadiki, M.; Ibnsouda, S. K. Methods for in Vitro Evaluating Antimicrobial Activity: A Review. *Journal of Pharmaceutical Analysis* **2016**, *6*, 71−79.
(27) Horn, M.; Reichart, F.; Natividad-Tietz, S.; Diaz, D.; Neundorf, I. Tuning the Properties of a Novel Short Cell-Penetrating Peptide by Intramolecular Cyclization with a Triazole Bridge. *Chem. Commun.* **2016**, *52* (11), 2261−2264.
(28) Scrima, M.; Le Chevalier-Isaad, A.; Rovero, P.; Papini, A. M.; Chorev, M.; D'Ursi, A. M. Cui Catalyzed Azide-Alkyne Intramolecular i-to-(I+4) Side-Chain-to-SideChain Cyclization Promotes the Formation of Helix-Like Secondary Structures. *Eur. J. Org. Chem.* **2010**, *2010* (3), 446−457.
(29) Tornøe, C. W.; Christensen, C.; Meldal, M. Peptidotriazoles on Solid Phase: [1,2,3]-Triazoles by Regiospecific Copper(I)-Catalyzed 1,3-Dipolar Cycloadditions of Terminal Alkynes to Azides. *J. Org. Chem.* **2002**, *67* (9), 3057−3064.
(30) D'Ercole, A.; Sabatino, G.; Pacini, L.; Impresari, E.; Capecchi, I.; Papini, A. M.; Rovero, P. On-Resin Microwave-Assisted Copper-Catalyzed Azide-Alkyne Cycloaddition of H1-Relaxin B Single Chain 'Stapled' Analogues. *Pept. Sci.* **2020**, *112* (4), No. e24159.
(31) Manning, M. C.; Woody, R. W. Theoretical CD Studies of Polypeptide Helices: Examination of Important Electronic and Geometric Factors. *Biopolymers* **1991**, *31* (5), 569−586.
(32) Has, C.; Das, S. L. The Functionality of Membrane-Inserting Proteins and Peptides: Curvature Sensing, Generation, and Pore Formation. *J. Membr. Biol. 2023 2564* **2023**, *256* (4), 343−372.
(33) Memariani, H.; Memariani, M. Antibiofilm Properties of Cathelicidin LL-37: An in-Depth Review. *World J. Microbiol. Biotechnol.* **2023**, *39*, 99.
(34) Lucana, M. C.; Arruga, Y.; Petrachi, E.; Roig, A.; Lucchi, R.; Oller-salvia, B. Protease-resistant Peptides for Targeting and Intracellular Delivery of Therapeutics. *Pharmaceutics* **2021**, *13* (12), 2065.
(35) Gaspar, D.; Veiga, A. S.; Castanho, M. A. R. B. From Antimicrobial to Anticancer Peptides. A Review. *Front. Microbiol.* **2013**, *4*, 294.
(36) Carrera-Aubesart, A.; Gallo, M.; Defaus, S.; Todorovski, T.; Andreu, D. Topoisomeric Membrane-Active Peptides: A Review of the Last Two Decades. *Pharmaceutics* **2023**, *15* (10), 2451.
(37) Nakamura, L. K.; Roberts, M. S.; Cohan, F. M. Relationship of Bacillus Subtilis Clades Associated with Strains 168 and W23: A Proposal for Bacillus Subtilis Subsp. Subtilis Subsp. Nov. and Bacillus Subtilis Subsp. Spizizenii Subsp. Nov. *Int. J. Syst. Bacteriol.* **1999**, *49* (3), 1211−1215.
(38) Cronenberg, T.; Hennes, M.; Wielert, I.; Maier, B. Antibiotics Modulate Attractive Interactions in Bacterial Colonies Affecting Survivability under Combined Treatment. *PLoS Pathog.* **2021**, *17* (2), No. e1009251.


https://doi.org/10.1021/acsinfecdis.4c00078
*ACS Infect. Dis.* XXXX, XXX, XXX−XXX